Data collapse of the spectra of water-based stable single-bubble sonoluminescence

Mogens T. Levinsen*
BioComplexity Laboratory, Niels Bohr Institute, Blegdamsvej 17, DK-2100 Copenhagen Ø, Denmark
(Received 9 March 2010; revised manuscript received 5 July 2010; published 29 September 2010)

In the early days of stable single-bubble sonoluminescence, it was strongly debated whether the emission was blackbody radiation or whether the bubble was transparent to its own radiation (volume emission). Presently, the volume emission picture is nearly universally accepted. We present new measurements of spectra with apparent color temperatures ranging from 6000 to 21 000 K. We show through data collapse that within experimental uncertainty, apart from a constant, the spectra of strongly driven stable single-bubble sonoluminescence in water can be written as the product between a universal function of wavelength and a functional form that only depends on wavelength and apparent temperature but has no reference to any other parameter specific to the experimental situation. This remarkable result does question our theoretical understanding of the state of the plasma in the interior of strongly driven stable sonoluminescent bubbles.

DOI: 10.1103/PhysRevE.82.036323 PACS number(s): 78.60.Mq, 44.40.+a, 52.35.Tc

I. INTRODUCTION

Soon after the first observation of stable single-bubble sonoluminescence (SBSL) [1,2], a controversy arose regarding the nature of its featureless spectrum (see, e.g., Ref. [3]). In stable SBSL a bubble of, e.g., air caught by a resonant sound field in a cell of water emits picosecond flashes of light in synchrony with the applied sound field. Let us emphasize here that by stable SBSL we mean flash-by-flash long-time (hours) stability in time as well as in space. Explicitly we exclude from the present analysis cases where transients play a role in creating the time-averaged spectrum. Thus re-entrant (recycling) bubbles as, e.g., in the experiment by Young *et al.* [4] as well as spatially unstable bubbles like the strongly emitting bubbles in sulfuric acid [5,6] are excluded from consideration. For simplicity we only consider strongly driven bubbles near the extinction boundary although we carefully avoid the regime where too high a gas concentration gives rise to spatial instabilities.

Since the spectrum of stable single-bubble sonoluminescence showed no emission or absorption lines, it was natural to compare it to blackbody radiation even though the quality of fits was not entirely convincing (see, e.g., Ref. [7]). This interpretation was abandoned for several reasons, and the prevailing theory is now that the bubble is transparent to its own emission. This is known as volume emission [3].

However, due to the resemblance to blackbody emission a best fit color temperature has often been used to characterize the spectra. In the present paper we shall present an investigation into how well this can be done. Thus we shall test whether a one-parameter functional form can be determined that within a constant amplitude factor specifies the shape of the spectra. To this end we look for a self-consistent way to write the raw spectra from a spectrometer as the product of a universal function of wavelength and a functional form of wavelength that only depends on temperature with all other parameters only entering through a species dependent amplitude constant. In essence whether all spectra can be written on the form

$$I_i(\lambda,T) = A_i g(\lambda) P(\lambda,T) \tag{1}$$

with A_i a species dependent constant, $g(\lambda)$ a universal function that only depends on the experimental environment, λ is the wavelength, and T is the color temperature associated with the bubble seeded with the species i.

II. BACKGROUND

There were several reasons why the interpretation of SSBL as blackbody radiation was abandoned. Assuming that the color temperatures [9] on the order of 10 000–20 000 K were indicative of spatially homogeneous bubble temperatures, conventional plasma physics calculations gave a mean free path for photons much larger than the bubble radius. This suggested that the bubble is transparent to its own radiation. A further complication arose when it became clear that the appearance of the red and blue parts of the spectrum was simultaneous. The possible generation of an internal shock wave by the violent collapse of the bubble offered one way to circumvent these problems. This mechanism would lead to strongly inhomogeneous heating and would raise the temperature in the core of the bubble by one or two orders of magnitude. The dominant emission might come from this opaque core.

A very careful study of this picture was presented by Moss *et al.* [10,11]. An important outcome of their work was that local temperature equilibrium is always established. Their study also considered the effects of water vapor caught in the bubble in the final stages of the collapse and showed that water vapor enhanced the possibility of an inhomogeneous temperature distribution in the bubble. The simulations of Moss *et al.* provided a first explanation of a prominent peak near 300 nm in the spectrum of a xenon bubble as due to the appearance of an opaque core in the bubble when the central temperature reached 0.9 eV ($\approx$10 000 K). Any further increase in the central temperature as the collapse intensified appeared only as an expansion of this region. The spectrum could thus be construed as the sum of a blackbody term from the surface of the core region and volume emission from the outer colder region.

*levinsen@nbi.dk

This effect was further shown to occur at a much higher temperature for argon with the opaque core correspondingly smaller. Consequently, the corresponding peak would be below 200 nm for the argon bubble spectrum. Although a smaller isentropic constant should lower the sound velocity in the gas and therefore favor diatomic molecules (and water) over the noble gases, the simulations by Moss *et al.* showed that the effect was virtually nonexistent for nitrogen. The simulated spectrum for nitrogen therefore increased all the way down to 200 nm.

The idea of a shock wave was later repudiated when dissipative effects were included and when simulations showed that the occurrence of shock waves was unlikely since even tiny deviations of the bubble from spherical symmetry would defocus a shock wave [12]. Predicted core temperatures were therefore reduced to the range of a few tens of thousand degrees Kelvin compared to the 10^8 K predicted by Wu and Roberts [13]. Apart from the continued attribution of the peak in the xenon spectrum to the existence of a small opaque core caused by a much gentler compression wave, the spectrum was now believed to be the result of volume emission. Various attempts have been made (see, e.g., Hammer and Frommhold [8]) to construct a spectrum *ab initio* by considering various bremsstrahlung mechanisms and recombination, but compelling results have not yet been obtained [14,15].

On the other hand, many experiments have been very difficult to explain on the basis of volume emission. This includes experiments on hydrogen bubbles, where the spectrum is nicely but not perfectly described by blackbody radiation [16]. Since this experiment stands alone, it has largely been disregarded by theoreticians. Furthermore, there are measurements of bubble anisotropy [17] and even anisotropic period doubling [18,19] seen directly in the light emission flash-by-flash. For reasons of symmetry [20] the latter phenomenon is extremely challenging. Finally, measurements of the size of the emitting core region of an argon bubble give a radius of approximately 0.25 μm, which is much smaller than the assumed size of the bubble [21]. In this connection let us also mention the molecular dynamics study by Bass *et al.* [22] that gives new theoretical life to the segregation picture.

The discussion of the origin of the SBSL spectrum has naturally been hampered by the fact that until recently only the noble gases with the exception of the relative newcomer hydrogen were shown to display stable sonoluminescence. In this respect an air bubble is actually an argon bubble with the stability directly linked to the presence of 1% argon in air ("the dissociation hypothesis" [3]). The problem with spectra from bubbles seeded with the noble gases is that they have rather similar color temperatures indicating a quite narrow range of bubble temperatures regardless of the origin of the spectra. This picture has now changed dramatically after it has been demonstrated that clean nitrogen bubbles also exhibit stable SBSL [23]. Note that this confirms the existence of the intermediate stability curve "B" postulated by Lohse *et al.* as a feature of the celebrated "dissociation hypothesis" [3]. In fact, even bubbles seeded by clean oxygen and also by mixtures of oxygen and nitrogen belong to the family of stable SBSL [23]. The spectra of these bubbles show much lower color temperatures than noble gas bubbles and thus provide us with a wider range for comparison with theory.

III. EXPERIMENTAL DETAILS

In the following, we compare spectra obtained from some noble and diatomic gases all driven at the high end of the stability range close to extinction. The inert gas bubbles are prepared from mixtures with 99% nitrogen while the diatomic gas bubbles are prepared from oxygen or nitrogen respectively with a content of noble gases below 10 ppm. The mixtures of inert gases (e.g., Ne-Xe) are approximately 50-50. The degas pressure for all cases was 260 ± 2 mbar corrected for water vapor pressure. The water temperature is 9.6 ± 0.3 °C for the measurements, and the atmospheric pressure ranged from 1003 to 1026 mbar although the variation under a single measurement is at most a few mbars.

The resonator, which is described in detail in Ref. [19], consists of a 6 cm high and 6 cm diameter quartz cylinder with metal caps at both ends. It is sealed using a pressure relief bag. Piezoelectric transducers are mounted on both caps for the drive, which has a frequency of approximately 21 930 Hz. A notable difference from these earlier experiments is the use of a heater as bubble initiator to avoid contamination with hydrogen. To avoid contamination with argon and traces of helium, the filtered water (0.2μ particle filter) was subjected to many hours of cycling between flushing with the gas in question and degassing in 15 min intervals. The final flushing at the desired concentration was done for 30 min. The water was violently agitated by a magnetic stirrer during the entire process.

The spectrum is measured using an Ocean Optics QE65000 fiber based spectrometer [charge coupled device (CCD) detector cooled to −10 °C] with a CC52 UV-NIR Miniature Light Collector/Collimator as front end. The entire system is calibrated in the 220–920 nm range with an Ocean Optics DH-2000-CAL NIST-traceable fiber based calibration source thereby producing a calibration table $I_{cal}(\lambda)$ for the spectrometer for post acquisition data processing.

Apart from supplying the color temperatures that are used as initial conditions, the calibration plays no further role in the analysis. This is performed on the original raw spectra after subtraction of the relevant background which has the obvious advantage of keeping the introduction of noise at a minimum.

IV. EXPERIMENTAL DATA

While in principle we can extend the analysis to all values of the drive where the criteria of stability is fulfilled, in the rest of the paper we shall only consider the properties of the spectrum at high drives.

The integration time for the noble gas spectra was 300 s, and the integration time for the diatomic gases was 10 000 s with background corrections using the same respective integration times. This gives an indication of the stability of these bubbles. Indeed the weather conditions in Copenhagen

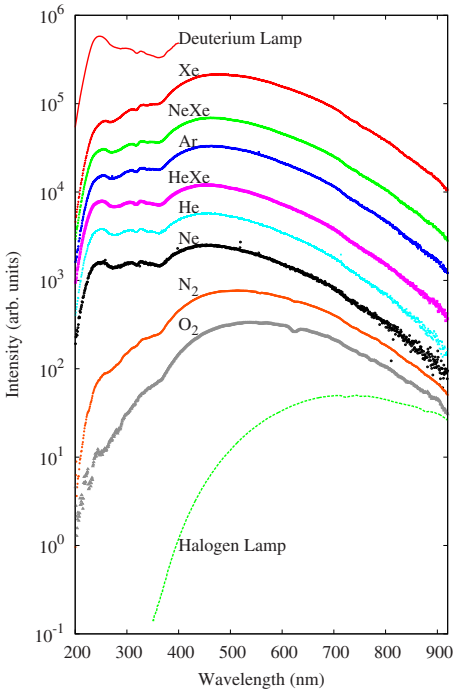

FIG. 1. (Color online) Raw spectra of some noble and diatomic gases. The uppermost truncated spectrum is the ultraviolet part of the spectrum of a deuterium lamp while the lowest spectrum is that of a halogen lamp. Spectra are displaced for clarity. (Displacement factors: Deuterium by 10, Xe by 10, NeXe by 4, Ar by 2.5, HeXe by 1.25, Halogen by 1/1000, the rest have no offset.)

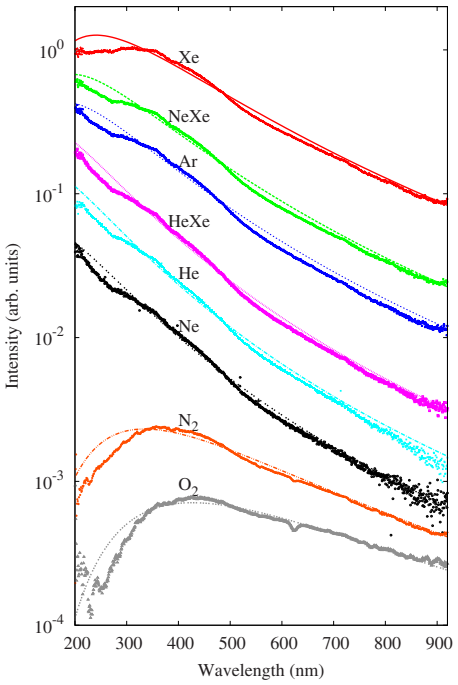

FIG. 2. (Color online) Calibrated spectra (points) of some noble and diatomic gases fitted to blackbody radiation I_{Planck} (lines). (Displacement factors: Xe by 10, NeXe by 4, Ar by 2.5, HeXe by 1.25, the rest have no offset.) The temperatures from the fits are Xe 12 000 K, NeXe 14 800 K, Ar 15 700 K, HeXe 20 400 K, He 20 800 K, Ne 20 000 K, N_2 8700 K, O_2 6800 K.

with new low pressure systems often passing on a daily basis pose the greatest problem for long-time stability of strongly driven bubbles.

The raw spectra do not seem to have any evidence of spectral lines in accordance with the observations of other investigators. However, some structure is clearly visible as evident from Fig. 1 where a collection of raw spectra all normalized to an integration time of 300 s is displayed. Common structure to the spectra is readily visible most prominently in the ultraviolet part of the spectrum but also in the far infrared while the rest of the spectrum from 380–700 nm is relatively featureless. An idea of the source of these structures is given by consideration of the two truncated spectra also displayed in Fig. 1. The uppermost is the ultraviolet part of the spectrum of a deuterium lamp while the lowest spectrum is that of a halogen lamp (divided by 1000 for clarity). Since clearly the observable structures are common to all spectra regardless of origin, they most likely are due to the overall response curve of the spectrometer set up. (The dip at 620 nm in the spectrum of the oxygen seeded bubble is a feature of the background spectrum and can also be distinguished in the nitrogen bubble spectrum but naturally appears weaker here by the ratio of the intensity of the spectra.)

The same collection of spectra are displayed in Fig. 2 but now with the calibration applied. The prominent "peak" in the xenon spectrum is quite notable. For comparison, we have fitted the spectra to that of blackbody radiation

$$I_{Planck}(\lambda,T) = C\frac{8\pi hc}{\lambda^5}\frac{1}{\exp(hc/\lambda k_B T)-1}, \qquad (2)$$

where h, c, and k_B are, respectively, Planck's constant, the speed of light, and Boltzmann's constant. T is the temperature of the blackbody emitter and λ the wavelength of the emitted light. As found by other authors, the overall fits for the noble gases are acceptable but not good. This statement is obviously also true for the spectra from diatomic gases. Note that the prefactor, C, would include information about pulse length and projected surface area of the emitting region if the spectra were truly blackbody.

However, if one looks closely it seems obvious that the calibration has not succeeded in removing all common structure. One might therefore wonder whether it is possible to find a single formula only depending on wavelength that would remove all common structure. Furthermore, in the spirit of using a color temperature to characterize the spectra, one might ask whether a functional form can be found that allows for a one-parameter representation of all spectra. In the following we shall analyze the data with this as a working hypothesis, and then test the resulting expression for self-consistency.

V. ANALYSIS

The question we pose is whether a functional form can be found that allows for a one-parameter representation of all spectra. Based on the above fit such a function must be remi-

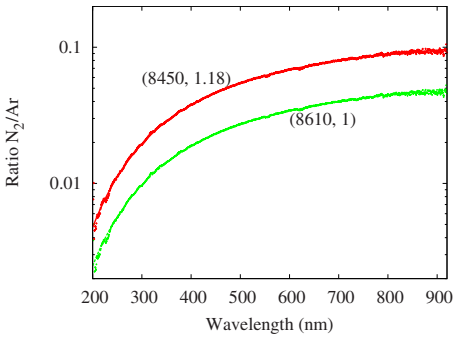

FIG. 3. (Color online) Upper red (dark gray) curves: Fit of the ratio between the nitrogen and the argon spectrum (+) to the corresponding ratio between the trial functions (line). Fit parameters $T=8450$ K, $k=1.18$. Lower green (light gray) curves: As above but with fit parameters $T=8610$ K, $k=1$, both lower curves offset by a common factor 0.5.

niscent of the Planck radiation formula. As a trial function we have therefore taken

$$I(\lambda,T)=A\frac{g(\lambda)}{\exp(hc/\lambda k_B T)-k}, \tag{3}$$

where T is the characterizing parameter and the constants A and k as well as the wavelength dependent function $g(\lambda)$ are to be determined by fitting. The function $g(\lambda)$ will of course include any multiplicative part of the true spectra that only depends on wavelength.

Choosing this particular form for the trial function constitutes so far only a mathematical convenience, not a necessity. Let us note here also that for instance the formula for free electron/ion bremsstrahlung [24] fails miserably (see Sec. VII for details). The data are processed in the following way. We start by assuming as characteristic parameter T_i for the spectrum of species i the value determined for T in the fit shown in Fig. 2. We form all possible ratios I_j/I_i between the raw spectra of species $j\neq i$ and the raw spectrum of species i. I_j/I_i is fitted to the corresponding ratios of the trial function with $a_j(i)=A_j/A_i$ (independent of λ), $k_j(i)$ and $T_j(i)$ as fitting parameters. Statistical weights based on count statistics are assigned to the experimental data to account for the noise in these.

Starting out with an argon spectrum where the characterizing temperature was determined as $T=17\,500$ K as suggested by the fit as above, we find, e.g., for the nitrogen spectrum displayed above the fitting parameters T and k to be 8450 K and 1.18, respectively. That the quality of the fit is quite good is seen from Fig. 3, where the ratios of the involved spectra together with the corresponding ratios of the trial functions are displayed. One immediately observes that the structures prominently present in the previous figures have disappeared thereby giving some support to the conjecture that the source of these structures is not intrinsic to sonoluminescence.

An interesting quantity is the average value $\langle k_j(i)\rangle = 1.02\pm 0.05$. That all ratios of spectra fit so closely to ratios between the trial function with just T as a parameter is in fact the crucial pivot point of the whole analysis. The close proximity to the blackbody value of 1 could now be used as justification for simply assuming $k=1$, essentially giving us a one-parameter functional form that apart from an undetermined prefactor, which presumably is a function of λ, is identical to the Planck radiation formula.

The corresponding fit for $k=1$ is also displayed in Fig. 3. For ease of comparison, the curves are displaced downward by multiplication with a common factor of 0.8. The variance of the two fits as defined by

$$\Delta=\frac{1}{N}\sqrt{\sum\left(\frac{y(\lambda)-I(\lambda,T)}{y(\lambda)}\right)^2}, \tag{4}$$

where N is the number of data points in the spectrum $y(\lambda)$, are, respectively, 0.0004 and 0.0005, thus remarkably close.

However, a more satisfying approach is the following. We construct the ratio between the raw spectrum I_j and the relevant trial function using all combinations $j\neq i$ with the corresponding fitting parameters, this construction being the correction needed in order to turn the raw spectra into exact fits to the corresponding trial function.

Using the maximum value of I_j with allowance for the difference in integration time as weights, we now determine a transformation function as an average of the ratios constructed above. The average transformation function $g(\lambda)$ will of course solely be a function of the wavelength.

In order to test in a self-consistent way whether the function $g(\lambda)$ is truly a universal function, we now apply the transformation to all raw spectra. As a last step in the procedure we fit the transformed spectra to the trial function but now with the parameter $k=1$ as suggested by the average value being so close to this value.

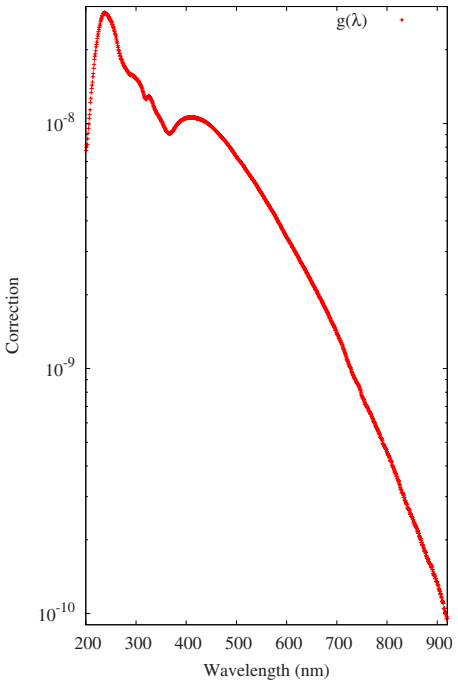

FIG. 4. (Color online) The function $g(\lambda)$ constructed from the fits as described in the text.

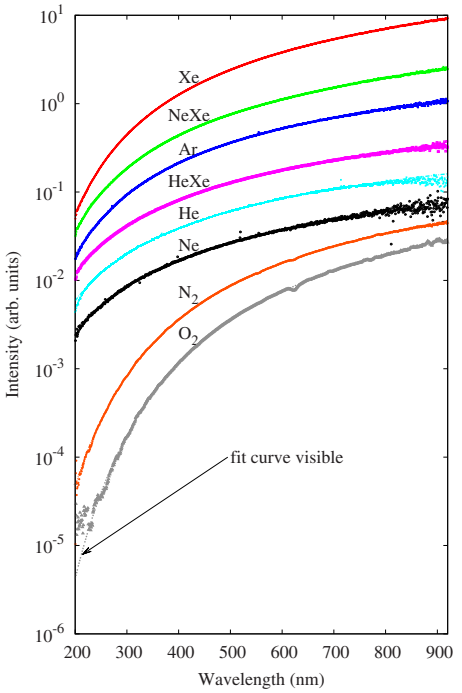

FIG. 5. (Color online) The raw spectra from Fig. 1 transformed by division with the universal function $g(\lambda)$. The spectra are fitted to the remaining part of the corresponding trial function. (Displacement factors: Xe by 10, NeXe by 4, Ar by 3, HeXe by 1.25, the rest have no offset.) The temperatures from the fits are Xe 11 810 K, NeXe 14 760 K, Ar 15 740 K, HeXe 20 380 K, He 20 840 K, Ne 19 990 K, N_2 8330 K, O_2 6440 K.

The final result for the function $g(\lambda)$ is displayed in Fig. 4, while Fig. 5 show the spectra after application of the transformation. In the same figure we have also displayed fits to the remaining part of the trial function setting $k=1$. As seen the fits are extraordinarily good. Also notice how all common structure has disappeared.

This actually constitutes a consistency check on the validity of the averaging procedure and the one-parameter description. The fitting curves can be distinguished from the data only at the extreme ends of the measured spectrum where noise can be observed due to the fall off in spectrometer sensitivity as observable from Fig. 1. Note that the featured argon spectrum was obtained more than 6 months later than that used in the construction of the universal function $g(\lambda)$, demonstrating the reproducibility of the measurements. Also note that the xenon bubble spectrum shows practically no deviation from the trial function, demonstrating that the "prominent peak" in the xenon spectrum is most likely due to a calibration error.

The temperatures obtained from the fit together with the prefactors are listed in Table I where the prefactors are relative to that of the argon spectrum in Fig. 2 using the argon spectrum as a reference point for convenience [25]. Let us note here that while the temperatures relative to each other are rather well determined, the absolute temperature scale has a much higher uncertainty. Ratios of spectra sufficiently different in color temperature can be fitted with both temperatures as independent parameters. A conservative estimate

TABLE I. Temperatures (K) and prefactors obtained by the trial function fits presented in Fig. 5.

	T (K)	Prefactor
Xe	11810 ± 8	3.33
Ne-Xe	14760 ± 13	1.52
Ar	15740 ± 12	0.82
He-Xe	20380 ± 40	0.42
He	20840 ± 100	0.24
Ne	19990 ± 50	0.11
N_2	8330 ± 7	0.35
O_2	6440 ± 13	0.40

relates the temperatures of Table I to the absolute temperature scale as $+20\%/-10\%$. Also note that while the weights, which the different spectra enter with in the derivation, are reflected in the relative sizes of the uncertainties for the temperatures of Table I, the values given here play no role in the determination of the average transformation function.

Another way to demonstrate the quality of the data collapse is to take the ratio of the spectrum of species j and the corresponding trial function. This is shown in Fig. 6.

To conclude this section we have shown that the spectra for a wide selection of species can be described by the product of a species dependent constant, a universal function $g(\lambda)$ that only depends on the wavelength λ and a one-parameter functional form that to all practical purposes is identical to the denominator of the Planck radiation formula. In the next section we shall discuss some of the implications of this analysis.

VI. DISCUSSION OF ANALYSIS

A natural extension, although the analysis does not provide any justification for this, would be to assume that the true functional form is identical to the Planck spectrum. This would mean multiplying both the transformed spectrum and the corresponding trial function without $g(\lambda)$ with λ^{-5}. Any discrepancies at the extreme ultraviolet end of the spectrum would be enhanced by this procedure, the result of which is shown in Fig. 7.

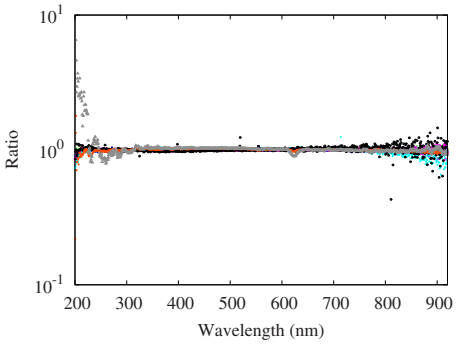

FIG. 6. (Color online) Data collapse of the ratio between the spectra and their corresponding trial function fits.

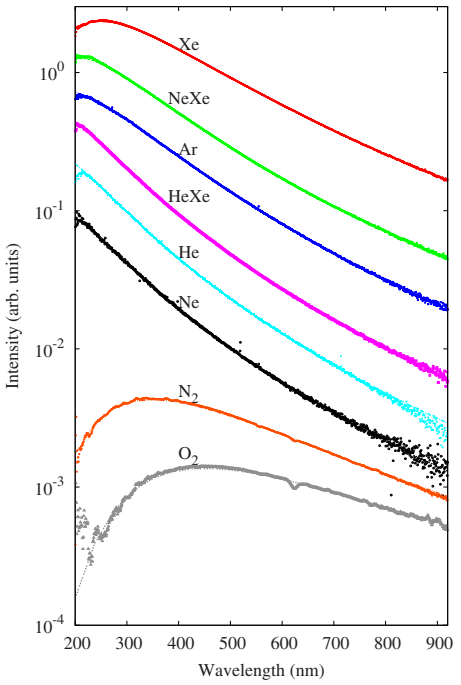

FIG. 7. (Color online) The transformed spectra and the corresponding trial functions without $g(\lambda)$, both multiplied with λ^{-5}.

Again we are confronted with an extraordinarily good agreement. It is therefore of interest to compare the actual calibration with the constructed formula to get an impression of the magnitude of the differences. But before doing this, it is appropriate to discuss the problems involved in performing the calibration.

As mentioned above the entire system is calibrated in the 220–920 nm range with an Ocean Optics DH-2000-CAL NIST-traceable fiber based calibration source thereby producing a calibration table $I_{cal}(\lambda)$ for the spectrometer. There are, however, several problematic issues that confound creating a perfect calibration table. The first concerns the geometry of the bubble environment. Since the output of the calibration lamp has to be delivered by an optical fiber at the position of the bubble we need to know the attenuation in the fiber. This is influenced by internal reflections which unfortunately depend on the medium surrounding the end of the fiber. Also the bubble is a point source whereas the output from the fiber is delivered inside a cone the opening angle of which depends critically on the output medium. Other problems relate to the interplay between the inherent structure in the lamp spectrum and structure in the response function of the spectrometer as only a finite amount of calibration points spaced 10 nm or more are supplied with the calibration lamps. This means some interpolation is needed. Finally one needs to measure the absorption in the water and glass wall of the vessel. As evidenced by the spectra published by Barber *et al.* [24] where structures common to all spectra are also clearly observable, getting a calibration good enough to settle without doubt the question of whether the spectra are truly blackbody is virtually impossible.

With this in mind we now make the comparison between the inverse of the transformation formula multiplied with λ^{-5} and the calibration table. This comparison is presented in Fig. 8.

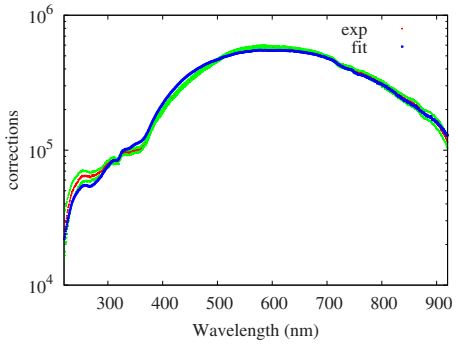

FIG. 8. (Color online) Comparison of the calibration and the transformation formula both multiplied with λ^{-5}. The red (middle light gray) curve is the calibration with the uncertainty indicated by the surrounding green (light gray) curves. The blue (solid black) curve is the transformation scaled to coincide with the calibration at 500 nm.

The uncertainty on the calibration is designated by the two accompanying curves. This represents the uncertainty determined from repeating the calibration procedure and thus does not include any possible systematic errors. With this in mind the deviation between the measured calibration and the transformation table is hardly great enough to rule out the possibility that the spectra are indeed described by the Planck formula.

VII. LOOK AT BREMSSTRAHLUNG

From a theoretical viewpoint, the formulas connected with bremsstrahlung whether from free electron/ion or free electron/neutral-atom interactions would constitute interesting choices as trial functions. Both processes can be expressed as follows [26–29]:

$$I(\lambda,T) \propto T^{\beta}\Gamma(\lambda,T)\exp(-hc/\lambda k_B T). \tag{5}$$

In the case of free electron/ion bremsstrahlung $\beta=-1/2$ and $\Gamma(\lambda,T)$ has the simple temperature independent form of λ^{-2}. Taking the ratio between any two spectra of this form would result in an exponential which in a semilogarithmic plot in frequency space would be represented by a straight line. Evidently not being the case for the experimental spectra, this particular form was rejected as a possible trial function.

Bremsstrahlung from electron interaction with neutral atoms is much more complicated since here $\Gamma(\lambda,T)$ is a species dependent function. Following Frommhold [30] using Eqs. (1) and (2) of this reference and the relevant tabulated momentum cross sections as supplied by Refs. [31,32], we have simulated some of the relevant spectra under the assumption that only the primary species participate in the emission. As in Ref. [30] we assume that the electron energy distribution is Maxwellian. For nitrogen and oxygen we have used the cross section for molecules. However, according to Kivel [33] the cross section for nitrogen atoms and molecules should only differ by a factor of two. This is presumably even more correct for oxygen. Nonetheless, even under these simplifying assumptions we are not able to get good

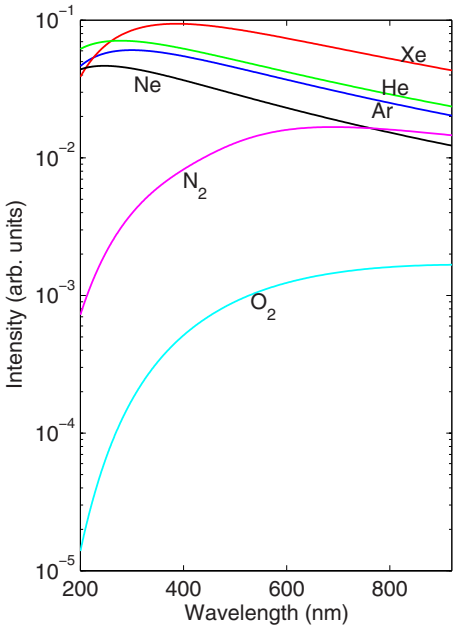

FIG. 9. (Color online) Electron/neutral-atom bremsstrahlung calculated for Ar (14 000 K), Xe (12 000 K), Ne (20 000 K), He (20 000 K), N_2 (8500 K), O_2 (6000 K) using realistic bubble temperatures taken from model calculations.

fits for the ratios without one temperature reaching extremely high values (of order a million degrees). Another serious problem is evident already from Ref. [30]. The spectra obtained from these simulations when compared to the calibrated spectra are much too flat when realistic temperatures taken from model calculations, see, e.g., Refs. [3,34], are employed. This is illustrated in Fig. 9 which should be compared with Fig. 2. As can be seen the simulations are generally off approximately by a factor λ^{-2}.

If temperatures on the other hand are raised in order to fit the calibrated spectra in the long wavelength regime, we no longer are able to reproduce the downward slope of the short wavelength regime. Furthermore, temperatures have to be raised to such high levels that the assumption of low electron concentration inherent in the electron/neutral-atom emission model is no longer valid. Indeed, the above arguments against both types of bremsstrahlung hinge on the assumption of a low level of ionization. If the ionization levels are high, we no longer can assume that the intensities are proportional to the absorption spectra calculated above. Instead we have to calculate the photon absorption coefficient κ_λ by multiplying the absorption spectra with the inverse Planck formula, the density of free electrons, and the density of atoms in the bubble [see Eq. (3), Ref. [30]]. The intensity is calculated by integrating the intensity at depth s, given by $I_{lambda}(s,T)=I_{Planck}(\lambda,T)[1-\exp(-\kappa_\lambda s)]$, over the volume of the bubble. If we only consider the main species as a source of free electrons, the density is for all reasonable temperatures so low that the bubble is transparent ($\tau_\lambda=2\kappa_\lambda R \ll 1$) and the intensity becomes proportional to the product τI_{Planck} [see Ref. [3], Eqs. (67)–(69)]. Thus we are left with the spectra being proportional to the absorption spectra calculated above and displayed in Fig. 9 with the additional problem that the spectra for nitrogen and especially oxygen becomes much too weak compared to the noble gas spectra even taking possible size and pulse length differences into account and using high density corrected ionization energies. Even assuming a water content of order 10% as responsible for contributing a majority of free electrons is not enough to alleviate this problem if a flat temperature profile is assumed.

However, let us emphasize that this does not imply that such processes are irrelevant. Only that if contributing, their imprint is masked in some fashion. Furthermore, as already noted by Frommhold [30], the high density encountered in the bubble may make many-body interactions very important changing the bremsstrahlung spectra considerably.

VIII. FUTURE WORK

The analysis strongly advocates some common ground for the radiation. The one mechanism already suggested, that might be in accordance with the whole palette of experimental results, is segregation of the gas in the bubble resulting in the lighter elements reaching a hotter core while leaving the heavier elements in the outer colder regions of the bubble. This could be in a mild form [35] as a result of a compressional wave inside the bubble or a more violent form [11] due to a shock wave. Suggested future work could therefore be along the lines of checking for the signature of segregation in the gradual change of spectra when the balance between light (e.g., helium or neon) and heavy (e.g., xenon) elements in mixtures of noble gases is shifted. Some work [36] have already been reported on this issue but the results are somewhat inconclusive as the authors only measured the total intensity as function of mixture content resulting the outcome being dependent on the response curve of the detector used. Also their degassing procedure did not ensure total removal of argon as is evident from the instabilities they observed for "pure" nitrogen bubbles which are now known to be stable when argon is completely removed [23]. To what degree small traces of argon may influence their results is unclear. One partial result of the present work is that a bimodal spectrum as suggested in Ref. [36] is not found for the mixtures used in the present work.

As water vapor or its reaction products surely would be involved in a segregation process, it would be relevant to extend the present study to higher ambient temperatures. This is unfortunately difficult with our present spectrometer due to the degradation of the signal to noise ratio with the much weaker signals. Finally, so far all experiments, as f.ex. anisotropic period doubling, that suggest the possible existence of a hot core are performed on air seeded bubbles. It would therefore be interesting to see whether anisotropic period doubling also takes place when the gas employed is either a heavy noble gas as xenon or especially a light noble gas as helium as the latter element is able to compete favorably with water vapor in reaching a possible hot core.

IX. CONCLUSION

To conclude, it is possible to express all spectra of strongly driven, long-time spatially and temporally stable,

sonoluminescent single bubbles of various noble and diatomic gases in water in a way that removes common structure from all. The crucial rational behind the construction is that all ratios between spectra are featureless and fit well to ratios between black body spectra. However, the construction of the transformation table does not hinge on this observation although it does present us with a logical choice of trial function and allow us to make better use of all information available. The procedure leaves behind smooth spectra that fit extraordinarily well to the temperature dependent part of the blackbody radiation formula without systematic deviations, regardless of gas content. This statement is based as well on the quality of the fits as on the glaring absence of structure in the experimental spectra after transformation with the result valid over an apparent temperature range of 6000–21 000 K.

As mentioned we cannot rule out *a priori* that common structure rooted in real physical processes could be removed by the process. The point here is that the revised "calibration" involves the multiplication of the raw spectra with a *universal* function that only depends on wavelength. This would place very restrictive bonds on the photon absorption coefficient κ_λ, whether the mechanism behind the emission is, e.g., bremsstrahlung, recombination, or radiative attachment. In the simple model of Brenner *et al.* [[3], Eq. (68)] for volume emission this would mean that κ_λ should be independent of seeding gas (except for this determining the temperature in the bubble). The only common species are hydrogen, oxygen, and nitrogen. Any emission or absorption lines should thus be related to these species but have the same relative strength in all cases to be suppressed. A candidate would be the OH line at 310 nm. However, the structure seen close to 310 nm is also present in the deuterium lamp spectrum and can thus be ruled out as being connected to the OH line. Altogether it is completely unlikely that species specific processes could contribute in a distinctive way in view of the range in apparent temperature and species involved.

We do not want to postulate that the spectra are true blackbody spectra in the sense of surface emission. However, the fact remains that any deviation from blackbody radiation has to be explicable in terms of a multiplicative function of wavelength alone with no dependence on bubble parameters such as species, internal temperature profile, optical depth etc. Furthermore, the observations reported here do not lend themselves to explanation by *any* of the existing theories of SBSL emission. Formally, we note that the purely experimental determination of absolute temperatures demands the availability of an extremely good calibration source. Indeed, the present results suggest that earlier difficulties in fitting the data to blackbody radiation may well be due to calibration errors.

ACKNOWLEDGMENT

The author acknowledges financial support from the Danish National Science Foundation.

[1] D. F. Gaitan, L. A. Crum, R. A. Roy, and C. C. Church, J. Acoust. Soc. Am. **91**, 3166 (1992).
[2] D. F. Gaitan, Ph.D. thesis, University of Mississippi, 1990.
[3] M. P. Brenner, S. Hilgenfeldt, and D. Lohse, Rev. Mod. Phys. **74**, 425 (2002).
[4] J. B. Young, J. A. Nelson, and W. Kang, Phys. Rev. Lett. **86**, 2673 (2001).
[5] D. J. Flannigan and K. S. Suslick, Phys. Rev. Lett. **95**, 044301 (2005).
[6] K. S. Suslick and D. J. Flannigan, Annu. Rev. Phys. Chem. **59**, 659 (2008).
[7] R. Hiller, S. J. Putterman, and B. P. Barber, Phys. Rev. Lett. **69**, 1182 (1992).
[8] D. Hammer and L. Frommhold, J. Mod. Opt. **48**, 239 (2001).
[9] By color temperature we understand the temperature derived from a best fit of a given spectrum to blackbody radiation, regardless of the origin of the spectrum.
[10] W. C. Moss, D. B. Clarke, and D. A. Young, Science **276**, 1398 (1997).
[11] W. C. Moss, D. A. Young, J. A. Harte, J. L. Levatin, B. F. Rozsnyai, G. B. Zimmerman, and I. H. Zimmerman, Phys. Rev. E **59**, 2986 (1999).
[12] A. K. Evans, Phys. Rev. E **54**, 5004 (1996).
[13] C. C. Wu and P. H. Roberts, Phys. Rev. Lett. **70**, 3424 (1993).
[14] W.-K. Tse and P. T. Leung, Phys. Rev. E **73**, 056302 (2006).
[15] Yu. An, Phys. Rev. E **74**, 026304 (2006).
[16] G. Vazquez, C. Camara, S. J. Putterman, and K. Weninger, Phys. Rev. Lett. **88**, 197402 (2002).
[17] K. Weninger, S. J. Putterman, and B. P. Barber, Phys. Rev. E **54**, R2205 (1996).
[18] J. S. Dam, M. T. Levinsen, and M. Skogstad, Phys. Rev. Lett. **89**, 084303 (2002).
[19] M. T. Levinsen, N. Weppenaar, J. S. Dam, G. Simon, and M. Skogstad, Phys. Rev. E **68**, 035303(R) (2003).
[20] Mogens T. Levinsen and Jeppe Seidelin Dam, *2006 Proceedings of ECC9* (Sao Jose dos Capos, Sao Paolo, 2006).
[21] J. S. Dam and M. T. Levinsen, Phys. Rev. Lett. **92**, 144301 (2004).
[22] A. Bass, S. J. Ruuth, C. Camara, B. Merriman, and S. Putterman, Phys. Rev. Lett. **101**, 234301 (2008).
[23] M. T. Levinsen and J. S. Dam, EPL **80**, 27004 (2007).
[24] B. P. Barber, R. A. Hiller, R. Löfstedt, S. J. Putterman, and K. R. Weninger, Phys. Rep. **281**, 65 (1997).
[25] In Ref. [16] the authors note that the apparent temperatures found by fits to blackbody radiation scale roughly with the ionization potentials of the relevant noble gases. Interestingly, oxygen and nitrogen are found to follow approximately the same scaling if instead the dissociation potentials are used. Whether this observation has any deeper meaning or just represents a coincidence is not clear.
[26] H. A. Kramers, Philos. Mag. **46**, 826 (1923).
[27] A. Unsöld, *Physik der Sternatmosphären* (Verlag von Julius Springer, Berlin, 1938).
[28] R. L. Taylor and G. Caledonia, J. Quant. Spectrosc. Radiat.

Transf. **9**, 657 (1969); **9**, 681 (1969).
[29] S. Geltman, J. Quant. Spectrosc. Radiat. Transf. **13**, 601 (1973).
[30] L. Frommhold, Phys. Rev. E **58**, 1899 (1998).
[31] L. G. H. Huxley and R. W. Crompton, *The Diffusion and Drift of Electrons in Gases* (Wiley, New York, 1974).
[32] R. B. Brode, Rev. Mod. Phys. **5**, 257 (1933).
[33] B. Kivel, J. Quant. Spectrosc. Radiat. Transf. **7**, 27 (1967).
[34] J. Holzfuss and M. T. Levinsen, Phys. Rev. E **77**, 046304 (2008).
[35] B. D. Storey and A. J. Szeri, J. Fluid Mech. **396**, 203 (1999).
[36] J. da Graça and H. Kojima, Phys. Rev. E **66**, 066301 (2002).